ACS APPLIED ENERGY MATERIALS

Article

Cite This: ACS Appl. Energy Mater. 2020, 3, 352−357

www.acsaem.org

Stability of Studtite in Aqueous Suspension: Impact of HCO_3^- and Ionizing Radiation on the Dynamics of Dissolution

Junyi Li, Annika C. Maier, and Mats Jonsson*

Department of Chemistry, School of Engineering Sciences in Chemistry, Biotechnology and Health, KTH Royal Institute of Technology, SE 10044 Stockholm, Sweden

ABSTRACT: In a geological repository for spent nuclear fuel, studtite $(UO_2)O_2(H_2O)_4$ may form on the fuel surface when in contact with groundwater under certain conditions. Studtite has a very low solubility and could thereby reduce the reactivity of spent nuclear fuel toward radiolytic oxidants. This would inhibit the dissolution of the fuel matrix and thereby also the spreading of radionuclides. It is therefore important to investigate the stability of studtite under conditions that may influence its stability. In this work we have studied the kinetics of studtite dissolution in aqueous suspensions containing no added HCO_3^- and with 10 mM HCO_3^-. The same type of experiment was performed also with solutions containing 0.2 mM H_2O_2. The solubility of studtite in the suspensions containing no added HCO_3^- is very low as expected, while the solubility in solutions containing 10 mM HCO_3^- is significantly higher. This is attributed to the formation of uranyl−carbonate and uranyl−peroxo−carbonate complexes. In 0.2 mM H_2O_2 and 10 mM HCO_3^- the observed solubility of U(VI) seems unaffected by the presence of H_2O_2. Again, this can be rationalized by the formation of uranyl−peroxo−carbonate complexes. It is interesting to note that H_2O_2 appears to be catalytically decomposed in solutions containing uranyl−carbonate complexes. In addition, γ-radiation-induced dissolution of studtite in HCO_3^- deficient solutions and in 10 mM HCO_3^- was studied. The dissolution rate was found to be extremely high in HCO_3^- under γ-irradiation. This is attributed to a combination of radiolytic degradation of H_2O_2 and the formation of uranyl−peroxo−carbonate complexes keeping the concentration of free H_2O_2 at a very low level and thereby driving the dissolution process.

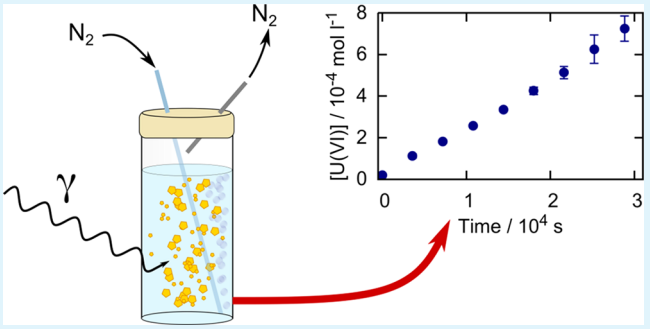

KEYWORDS: *studtite, dissolution, spent nuclear fuel, radiolysis, hydrogen peroxide, uranyl complexes*

INTRODUCTION

In several countries, deep geological repositories are considered the safest alternative for long-term disposal of spent nuclear fuel. Given the enormously long-time spans during which the integrity of the barriers used in the repository must remain intact to guarantee the safety of the repository, it is of utmost importance to study every possible process that could affect the barriers. To be able to assess the consequences of multiple barrier failure, it is also essential to study the kinetics and mechanisms of processes that could occur when the spent nuclear fuel comes in contact with groundwater, in particular processes that affect the spreading of radionuclides from the spent nuclear fuel. The most common types of commercial nuclear fuel are based on UO_2, and since the fissile fraction of uranium in the fuel is fairly low, UO_2 is also the main constituent of the spent nuclear fuel. In addition to UO_2, spent nuclear fuel contains ca. 5% radioactive fission products and heavier actinides.[1] Radiotoxic nuclides are assumed to be released to the groundwater, mainly upon dissolution of the UO_2−matrix.[2,3] At potential deep geological repository sites, the groundwater is usually reducing, and under these conditions the solubility of UO_2 is very low.[3] However, the ionizing radiation emitted from the spent nuclear fuel will be absorbed by the groundwater, resulting in water radiolysis. Radiolysis of water produces oxidants ($HO^\bullet$, H_2O_2, and $HO_2^\bullet$) as well as reductants (e_{aq}^-, $H^\bullet$, and H_2).[4] For kinetic reasons, the surface reactions will, at least initially, be dominated by the oxidants which drastically increase the solubility of the UO_2−matrix (U(VI) being several orders of magnitude more soluble than U(IV)).[5] The dissolution process is further accelerated by the common groundwater constituent HCO_3^- since UO_2^{2+} readily forms highly soluble carbonate complexes.[6] Among the radiolytic oxidants, H_2O_2 has been shown to dominate the oxidative dissolution of UO_2 under repository conditions.[5]

H_2O_2 can react with UO_2^{2+} to form studtite, $(UO_2)O_2(H_2O)_4$, or its dehydration product metastudtite, $(UO_2)O_2(H_2O)_2$. These two phases have very low solubilities, and from a strictly thermodynamic point of view,[7] studtite should be formed upon oxidation of UO_2 by H_2O_2 even in the presence of HCO_3^- although this has, to the best of our knowledge, never been reported. However, in HCO_3^- deficient systems, studtite or metastudtite was found to precipitate on

Received: August 17, 2019
Accepted: December 9, 2019
Published: December 9, 2019

DOI: 10.1021/acsaem.9b01611
ACS Appl. Energy Mater. 2020, 3, 352−357

the surface of UO_2 and thereby reduce its reactivity.[8,9] In the presence of H_2O_2 studtite formation is thermodynamically favorable over formation of uranyl oxide hydrates and uranyl silicates.[10] The existence of studtite and metastudtite on the surface of commercial spent nuclear fuel was confirmed by Hanson et al. after immersing fuel fragments in deionized water over 2 years at room temperature. In their experiments, X-ray diffraction (XRD) showed that studtite and UO_2 were the major phases in all the samples, while metastudtite was only identified in the solids floating at the sample air−water interface.[11] The source of H_2O_2 in these experiments was water radiolysis. Moreover, oxidative dissolution experiments on UO_2 were performed by Clarens et al.[8] and have shown that at a low H_2O_2 concentration (5×10^{-3} mM), the uranium concentration increased as a function of time. However, at a higher H_2O_2 concentration (0.5 mM), a steady-state concentration of uranium as well as a yellow precipitate were observed. The latter was identified as studtite. Hence, the formation of studtite on the surface of spent nuclear fuel could affect the long-term stability of spent nuclear fuel in a repository after the intrusion of groundwater. Recently, Kim et al. studied the kinetics of studtite dissolution under various conditions of geochemical relevance.[12]

It is interesting to note that even though the solubility of studtite is quite low in general, there is a growing body of evidence showing that nanocluster formation can efficiently solubilize studtite under certain conditions.[13,14] Uranyl peroxide nanoclusters can also be formed from other solid uranium compounds than studtite.[15]

In addition, uranyl has been shown to form various complexes with hydrogen peroxide and carbonate.[16] Interestingly, the presence of carbonate prevents the formation of larger clusters.[16]

In this work, the dissolution dynamics of studtite in HCO_3^- deficient and 10 mM HCO_3^- solution have been studied experimentally to assess the impact of HCO_3^-. The released H_2O_2 and U(VI) were monitored as a function of time. Moreover, the influence of H_2O_2 on the stability of studtite as well as the influence of studtite on the stability of H_2O_2 were investigated experimentally. To study the effects of irradiation, dissolution experiments in the presence and absence of HCO_3^- under continuous exposure to γ-radiation were conducted.

EXPERIMENTAL SECTION

All solutions used during the experiments were prepared using Milli-Q water (18.2 MΩ cm). Chemicals were of reagent grade unless otherwise stated.

The concentrations of H_2O_2 were measured using the Ghormley triiodide method where I^- is oxidized to I_3^- by H_2O_2.[17,18] The absorbance of I_3^- was measured at λ = 360 nm by UV/vis spectrophotometry.

The concentrations of U(VI) were measured using the Arsenazo III method,[19] where uranyl forms a complex with the Arsenazo III reagent in acid media. The absorbance of the complex is measured at λ = 653 nm by UV/vis spectrophotometry.

Synthesis of Studtite. For each individual experiment a batch of 40 mg of studtite was precipitated from aqueous solution by adding 40 mM H_2O_2 to 4.3 mM uranyl nitrate ($UO_2(NO_3)_2{\cdot}6H_2O$). The uranyl solution was prepared by dissolving 54 mg of uranyl nitrate in 25 mL of water with an initial pH of 3.5 (acidified by HCl).[20] An excess of H_2O_2 was used to maximize product formation.[21] The synthesis was carried out at room temperature with stirring for 24 h and was protected from light. After the synthesis, the uranyl concentrations were measured and found to be below the detection limit of the method. The synthesized studtite powder was washed twice with water to remove the remaining H_2O_2 and unreacted uranyl nitrate. During each washing step, the original liquid was replaced with 25 mL of water. Afterward, the suspension was left to resediment overnight before the second washing step.

Solid Phase Characterization. Synthesized studtite was characterized using powder X-ray diffraction (XRD). XRD patterns were recorded at room temperature on a PANalytical XPert PRO diffractometer using a Bragg−Brentano geometry and Cu Kα radiation (1.5418 Å) in a 2θ range between 10°and 110°. The powder sample was grounded manually in an agate mortar, and a silicon wafer was used as sample holder.

Studtite Dissolution Kinetics. After washing each 40 mg studtite batch with water (as described above), we replaced the excess solution once more with 25 mL of aqueous solution containing no added HCO_3^- or containing 10 mM HCO_3^- (the latter was added to the solution after weighing an appropriate amount of $NaHCO_3$). Immediately after adding the aqueous solution, we measured the concentrations of H_2O_2 and U(VI) as a function of time. Each sample container was sealed with a rubber septum and continuously purged with N_2 at room temperature. For each H_2O_2 and U(VI) measurement, 1.5 mL of aliquots were taken from the studtite suspension and filtered through 0.2 μm cellulose acetate syringe filters. For each measurement, the H_2O_2 and U(VI) determinations were done in duplicate. The difference between the duplicate measurements was less than 4.5 μM and 14 μM, respectively, for H_2O_2 and U(VI). All experiments were performed at least three times. The error bars in the figures reflect the results of these experiments and are based on the standard deviation derived from the three repetitions of each experiment.

The influence of H_2O_2 on the studtite dissolution kinetics in bicarbonate-deficient and 10 mM bicarbonate solutions was studied by adding H_2O_2 to a concentration of 0.2 mM at the start of the experiment.

The pH values of the solutions were measured before and after each experiment. No buffer was added to the solutions without added HCO_3^-.

Irradiation Experiments. γ-Irradiation experiments were carried out after adding 25 mL of aqueous solution containing no added or containing 10 mM HCO_3^- to the washed precipitate. The glass vials containing the aqueous powder suspensions were sealed by rubber septa and irradiated in a Cs-137 gamma source for 8 h (Gammacell 1000 Elite, MDS Nordion). The dose rate of 0.11 Gy s^{-1} was determined by Fricke dosimetry.[4] All suspensions were continuously purged with N_2 or N_2O. Next, 1.5 mL aliquots were taken from the powder suspensions before irradiation and then every hour to measure the concentrations of H_2O_2 and U(VI). The pH values of the solutions were measured before and after exposure to ionizing radiation.

RESULTS AND DISCUSSION

Solid Phase Characterization. The solid product from the synthesis was originally dried in a glovebox under Ar atmosphere. To assess the impact of the atmosphere during drying, we also dried solid samples in air at room temperature for 24 h. The resulting powder XRD patterns are shown in Figure 1.

It is interesting to note that the sample dried in the glovebox under Ar atmosphere is identified as metastudtite while the sample dried in air is identified as studtite. The reason for forming metastudtite when drying the solid in the glovebox is probably the extremely dry (low humidity) atmosphere of the glovebox that promotes dehydration of the product.

Studtite Dissolution Kinetics. As the synthesized solid was washed but not dried prior to the dissolution experiments, there was no risk of converting studtite into metastudtite. The results of the dissolution experiments performed in aqueous

DOI: 10.1021/acsaem.9b01611
ACS Appl. Energy Mater. 2020, 3, 352−357

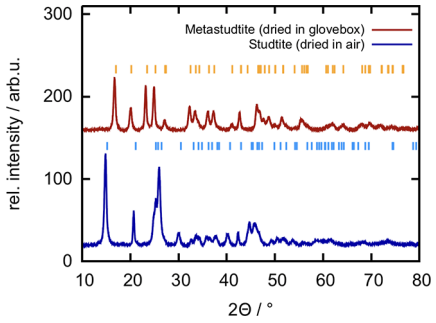

Figure 1. Powder XRD patterns of solid samples dried in a glovebox under Ar (red) and in air (blue). Indexes for studtite from ref 22 and for metastudtite from ref 23.

suspensions containing no added HCO_3^- and containing 10 mM HCO_3^- are summarized in Figure 2.

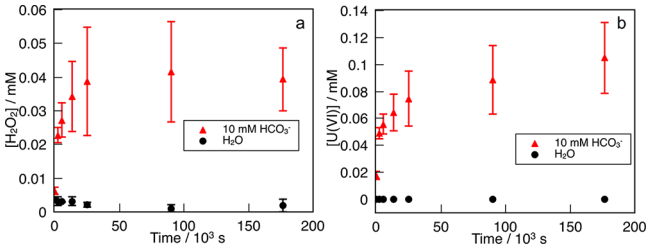

Figure 2. $[H_2O_2]$ (a) and [U(VI)] (b) as a function of time for aqueous studtite powder suspensions containing no added HCO_3^- (black dots) or added 10 mM HCO_3^- (red triangles).

As expected, there is a clear difference in dissolution behavior of studtite depending on the presence of HCO_3^-. In the solution without added HCO_3^-, the initial pH was 5.42 and it remained constant throughout the experiment. In the solution containing 10 mM HCO_3^-, the initial pH was 8.47, and the pH at the end of the experiment was 9.47. In the absence of HCO_3^-, the concentrations of H_2O_2 and U(VI) are close to the detection limits, and it is not possible to assess any dissolution dynamics. This is well in line with the very low solubility previously reported.[7] However, for studtite in 10 mM HCO_3^-, dissolution occurs at an appreciable rate as demonstrated by the increase in concentrations of H_2O_2 and U(VI). This can partly be attributed to the formation of soluble complexes between U(VI) and carbonate/bicarbonate but also to the formation of uranyl−peroxo−carbonate complexes. The expected solubility only taking the uranyl−carbonate complex into account can be calculated from the solubility product of studtite ($\log K_{sp} = -2.88$)[7] in combination with the carbonate complexation equilibrium constant ($\log K = 21.84$ for $UO_2(CO_3)_3^{4-}$)[24] and the pK_a of HCO_3^- (10.33). Under the present conditions, the solubility of studtite is calculated to be approximately 40 μM. However, the actual solubility accounting also for the uranyl−peroxo−carbonate complexes is higher. The increased solubility under these conditions can mainly be attributed to $(UO_2)_2(O_2)(CO_3)_4^{6-}$ and $(UO_2)(O_2)(CO_3)^{2-}$.[16] The solubility based on the carbonate complex alone is well in line with the measured H_2O_2 concentration but is lower than the measured U(VI) concentration. It should be pointed out that the solid phase is not quantitatively dissolved in the suspension containing 10 mM HCO_3^- (less than 3% is dissolved). In the recent work by Kim et al.[12] the solubility of studtite under the same conditions as here is reported to be ca. 45 μM, which corresponds very well to the thermodynamical solubility taking only the uranyl−carbonate complex into account. However, it should be noted that Kim et al. only measured the concentration of dissolved uranium (not H_2O_2) and that the amount of studtite in relation to the solution volume used in their experiments is much lower than in this work. In fact, if all of the studtite was dissolved in their experiments, the uranium concentration would be 54 μM. This is only slightly above the calculated solubility. Kim et al. also studied the dissolution of studtite as a function of HCO_3^- concentration from 10^{-4} to 10^{-2} M. Judging from the figures they present, increasing the HCO_3^- concentration from 10^{-4} to 10^{-3} M increases the initial rate of dissolution by almost a factor of 10. However, increasing the HCO_3^- concentration from 10^{-3} to 10^{-2} M increases the initial rate of dissolution by more than two orders of magnitude. As pointed out by the authors, the trend can be attributed to the fact that $UO_2(CO_3)_2^{2-}$ is the dominating complex at $[HCO_3^-] = 10^{-4}$ M while $UO_2(CO_3)_3^{4-}$ dominates at $[HCO_3^-] \geq 10^{-3}$ M. This could explain why the concentration dependence on the kinetics changes.

The rate of dissolution (in M s^{-1}) at 10^{-2} M HCO_3^- appears to be higher in the present work in comparison to the work by Kim et al.[12] This is most probably attributed to the significantly larger surface area to solution volume ratio used in the present work (assuming similar specific surface areas for the synthetic studtite).

In the present experiments, H_2O_2 appears to have reached a maximum concentration already within 7 h, whereas the U(VI) concentration keeps increasing throughout the experiment. The ratio between the concentrations of H_2O_2 and U(VI) upon dissolution of studtite should be 1:1. The fact that the U(VI) concentration is more than twice as high as compared to H_2O_2 implies that H_2O_2 is consumed in the system. The postulated consumption of H_2O_2 in the system would contribute to further dissolution of studtite from a strictly thermodynamical point of view. It should be noted that the formation of soluble uranyl−peroxide nanoclusters has only been observed in alkaline solutions (pH > 12) and in solutions containing very high concentrations of H_2O_2 at slightly lower pH (>10).[25−27] Hence, it is very unlikely that cluster formation contributes to the dissolution of studtite under the conditions used in this work.

The Influence of H_2O_2 on Studtite Dissolution. Given that the dissolution equilibrium only accounts for the formation of uranyl−carbonate complexes, the presence of H_2O_2 would be expected to suppress the dissolution of studtite also in HCO_3^- containing solution. The results from dissolution experiments performed with an initial H_2O_2 concentration of 0.2 mM are presented in Figures 3a and 3b.

Figure 3a shows the dissolution kinetics of studtite in 0.2 mM H_2O_2 in the absence of added HCO_3^-. As can be seen, the concentration of U(VI) is close to the detection limit (1 μM) and does not increase with time. The H_2O_2 concentration remains constant at about 0.2 mM. This shows that the studtite surface is not an active catalyst for H_2O_2 decomposition. Numerous oxide surfaces, including UO_2, have been shown to catalyze the decomposition of H_2O_2 to H_2O and O_2 with the intermediate formation of surface-bound hydroxyl radicals.[28−30] The present results imply that covering the UO_2 surface with studtite would reduce the surface reactivity toward H_2O_2.

DOI: 10.1021/acsaem.9b01611
ACS Appl. Energy Mater. 2020, 3, 352−357

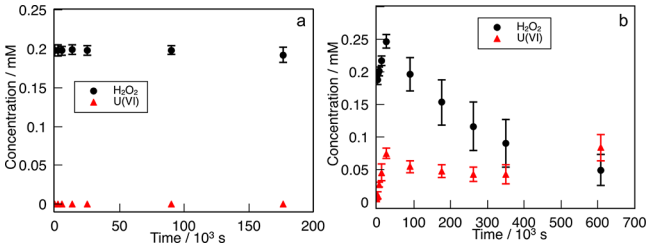

Figure 3. Concentrations of H_2O_2 (black dots) and U(VI) (red triangles) as a function of time for aqueous studtite powder suspensions containing no added HCO_3^- and 0.2 mM H_2O_2 (a) and containing 10 mM HCO_3^- and 0.2 mM H_2O_2 (b).

Figure 3b shows the dissolution kinetics of studtite in 10 mM HCO_3^- and an initial H_2O_2 concentration of 0.2 mM. Both the concentrations of H_2O_2 and U(VI) reach a maximum within 7 h, and the maximum concentration of dissolved U(VI) is almost the same as in the absence of initial H_2O_2. Hence, the solubility of studtite would appear to be independent of the H_2O_2 concentration, which is indeed unexpected if only the uranyl−carbonate complex is considered. From the known equilibrium constants we can calculate the solubility under the present conditions to be approximately 7 μM, which is almost one order of magnitude below the observed U(VI) concentration. However, if formation of uranyl−peroxo−carbonate complexes is also considered (primarily $(UO_2)(O_2)(CO_3)^{2-}$ and $(UO_2)(O_2)(CO_3)_2^{4-}$),[16] the experimentally observed concentrations are not unreasonable. Interestingly, both the concentrations of U(VI) and H_2O_2 decrease after reaching a maximum. The decrease in U(VI) concentration is moderate while the H_2O_2 concentration is reduced by 80% during the time of the experiment.

To explore the reason why the H_2O_2 released during studtite dissolution in HCO_3^- is slowly consumed, we prepared three different types of solutions and measured the concentrations of H_2O_2 as well as U(VI) (when applicable) over time. The first set of solutions contained 0.05 mM $UO_2(NO_3)_2$ and 0.1 mM H_2O_2 in 25 mL of 10 mM HCO_3^-. The second set of solutions contained 0.1 mM H_2O_2 in 25 mL of 10 mM HCO_3^-. In the third set of solutions, 0.1 mM $NaNO_3$ and 0.1 mM H_2O_2 were added to 25 mL of 10 mM HCO_3^-. The results for set number 1 can be seen in Figure 4.

As can be seen in Figure 4, H_2O_2 is almost completely consumed during the time frame of the experiment. It should be noted that no significant H_2O_2 consumption can be observed for samples not containing U(VI) (i.e., in the second and third sets of solutions, data not shown). Hence, H_2O_2 must be considered stable at the present pH and HCO_3^- concentration. What is really interesting here is the fact that the U(VI) concentration remains constant throughout the experiment, implying that the uranyl−carbonate complex acts as a catalyst for H_2O_2 decomposition. Further studies of this reaction are currently underway.

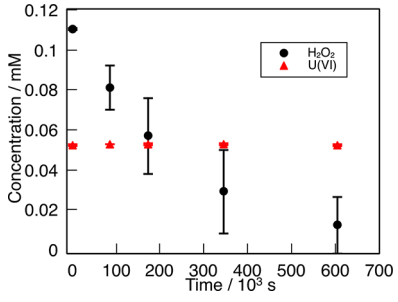

Figure 4. H_2O_2 and U(VI) concentrations as a function of time in an aqueous solution originally containing 0.1 mM H_2O_2, 0.05 mM U(VI), and 10 mM HCO_3^-.

Kim et al. also studied the influence of H_2O_2 on the dissolution of studtite.[12] They used aqueous solutions spiked with 10^{-3}, 10^{-2}, and 10^{-1} M H_2O_2. The results show increasing initial dissolution with increasing H_2O_2 concentration followed by a slower decrease in uranium concentration. Interestingly, the fastest initial dissolution and the highest concentration of dissolved uranium were observed at a very high H_2O_2 concentration. Under similar conditions, soluble uranyl−peroxide nanoclusters have been shown to form, provided that the pH is high enough.[31]

γ-Irradiation Experiments. The concentrations of U(VI) and H_2O_2 as a function of irradiation time for aqueous suspensions of studtite continuously purged with N_2 are presented in Figure 5.

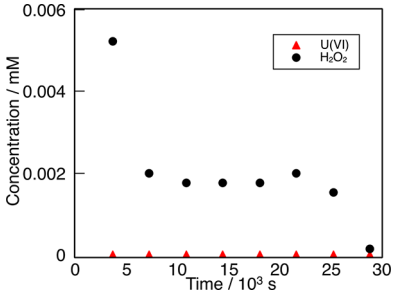

Figure 5. Concentrations of H_2O_2 (black dots) and U(VI) (red triangles) as a function of irradiation time for aqueous studtite powder suspensions (0 mM HCO_3^-) exposed to γ-radiation.

As can be seen, the concentrations of H_2O_2 and U(VI) do not increase after 8 h, indicating that the solubility of studtite is very low in pure water also when exposed to γ-radiation. The detection limit for H_2O_2 is around 5 μM and for U(VI) it is around 1 μM. Hence, the concentrations in Figure 5 are, in general, below the detection limit, and the apparent changes in the H_2O_2 concentration with time are insignificant.

The results from the corresponding experiments using aqueous solutions containing 10 mM HCO_3^- are presented in Figures 6a and 6b, together with the corresponding data for the unirradiated suspensions.

The results are truly intriguing as it is quite clear that irradiation of the suspensions has a dramatic impact on the dissolution of studtite. After 8 h of irradiation, the U(VI)

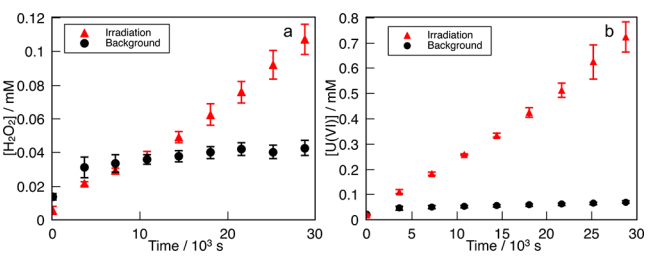

Figure 6. Concentration of H_2O_2 (a) and U(VI) (b) as a function of time for irradiated (red triangles) and unirradiated (black dots) aqueous studtite powder suspensions containing 10 mM HCO_3^-.

DOI: 10.1021/acsaem.9b01611
ACS Appl. Energy Mater. 2020, 3, 352−357

concentration (0.72 mM) is approximately 10 times higher than that in the absence of irradiation (0.07 mM). The concentration of H_2O_2 is also higher in the irradiated system as compared to the unirradiated system but only by a factor of 3. It is also quite clear that the concentration of U(VI) in the irradiated solution is about seven times higher than the concentration of H_2O_2 in the same solution. In the unirradiated solution the corresponding ratio is around two. The pH value of the solution before irradiation was 8.47, and the pH value after irradiation was 9.91. The relatively low H_2O_2 concentrations compared to U(VI) can partly be explained by H_2O_2 reacting with the aqueous radiolysis products. In fact, when performing a numerical simulation of the radiation chemistry of water assuming the release of H_2O_2 (in addition to radiolytically formed H_2O_2) to occur at the same rate as the release of uranium and using the dose rate of the experiment, the predicted evolution of the H_2O_2 concentration in solution is fairly close to the experimentally observed trend. However, the high concentrations of U(VI) in the irradiated system cannot be attributed to the solubility of studtite taking only the uranyl−carbonate complex into account.

To try to shed some light on the mechanism of the radiation-induced dissolution of studtite, we repeated the experiment purging with N_2O instead of N_2. In N_2O-saturated solutions, the hydrated electron is rapidly converted to a hydroxyl radical according to reactions 1 and 2.[32]

$$e^-_{aq} + N_2O \rightarrow N_2 + O^{\bullet -} \quad (1)$$

$$O^{\bullet -} + H_2O \rightarrow HO^{\bullet} + HO^- \quad (2)$$

Hence, the yield of reducing radicals is drastically reduced while the yield of hydroxyl radicals is doubled. In a solution containing HCO_3^-, the hydroxyl radical is converted into carbonate radical anions ($CO_3^{\bullet -}$). In other words, purging with N_2O will change the chemical conditions significantly. A possible reason for the radiation-induced dissolution of studtite could be a reaction between studtite and the hydrated electron reducing the peroxide moiety of studtite and thereby solubilizing the uranyl. If this process is indeed responsible for the observed dissolution, the experiment with N_2O purging will display slower dissolution. The results are presented in Figures 7a and 7b.

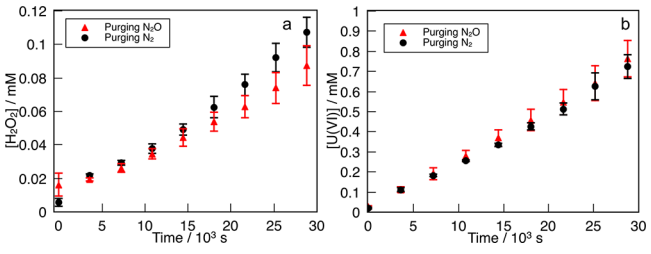

Figure 7. Concentration of H_2O_2 (a) and U(VI) (b) as a function of irradiation time for aqueous studtite powder suspensions containing 10 mM HCO_3^- purged with N_2O (red triangles) and N_2 (black dots).

As can be seen in Figures 7a and 7b, there are no significant differences in either the H_2O_2 concentrations or the U(VI) concentrations between the N_2O- and the N_2-purged suspensions. This clearly shows that the hydrated electron is not involved in the dissolution process. It is difficult to imagine that a radiolytic oxidant would be responsible for the dissolution as studtite is already oxidized. Nevertheless, doubling the yield of oxidative radicals does not have an appreciable effect on the dissolution. Another plausible reason would be direct absorption of the radiation energy by the solid. To investigate this, three samples of 40 mg of studtite powder each were dried in air, and then two of the samples were irradiated for 8 h (corresponding to 3.2 kGy). One dried and irradiated sample was taken for powder XRD analysis. The XRD pattern shows that there was no detectable change in the studtite crystal structure or in its crystallinity. While for the two other samples (one irradiated and one unirradiated), 25 mL of aqueous solution containing 10 mM HCO_3^- was added, and the H_2O_2 and U(VI) concentrations were monitored over time. The results are presented in Figures 8a and 8b.

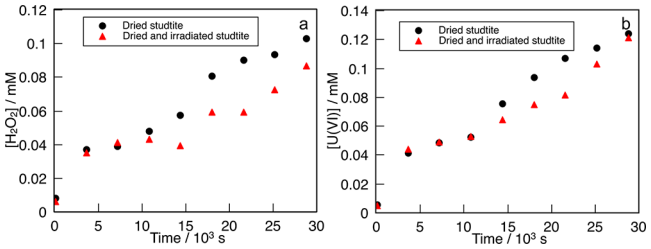

Figure 8. H_2O_2 (a) and U(VI) (b) concentrations as a function of time for dried (black dots) and dried and irradiated (red triangles) studtite powders immersed in aqueous solutions containing 10 mM HCO_3^-.

As can be seen in Figures 8a and 8b, the differences in H_2O_2 and U(VI) concentrations between the irradiated and unirradiated samples are very small. This implies that the relatively extreme dissolution observed for studtite suspensions containing HCO_3^- continuously exposed to γ-radiation cannot be attributed to permanent chemical changes due to direct absorption of the radiation by the solid. This is further evidenced by the fact that dry irradiation of studtite does not induce detectable changes in the XRD pattern. It is important to note that radiation enhanced dissolution of studtite is only observed for suspensions containing HCO_3^-. Since changing the gas atmosphere from N_2 to N_2O has an insignificant effect on the dissolution kinetics, we can rule out the active involvement of e^-_{aq} as well as $CO_3^{\bullet -}$ in this process.

Given the experimental observations presented above, the high U(VI) concentrations obtained upon irradiation of aqueous studtite suspensions containing HCO_3^- can most probably be explained by the increase in pH which drastically increases the stability of some of the uranyl−peroxo−carbonate complexes (mainly $(UO_2)(O_2)(CO_3)_2^{4-}$)[16] and thereby reduces the concentration of free H_2O_2 to very low levels. The direct consequence of this is that the solubility of studtite increases. Hence, the combination of radiolytic degradation of H_2O_2 and formation of uranyl−peroxo−carbonate complexes keeps the concentration of free H_2O_2 at a very low level and thereby drives the dissolution process.

These results clearly show that radiation driven dissolution of studtite would have a significant impact on the stability of studtite under deep repository conditions.

CONCLUSIONS

The present work shows that the solubility of studtite in the suspensions without added HCO_3^- is very low. In suspensions containing 10 mM HCO_3^-, the observed solubility is

DOI: 10.1021/acsaem.9b01611
ACS Appl. Energy Mater. 2020, 3, 352−357

considerably higher. This is attributed to the formation of uranyl−carbonate and uranyl−peroxo−carbonate complexes. In the presence of 0.2 mM H_2O_2 and 10 mM HCO_3^- the solubility is higher than expected if only the carbonate complex is accounted for but reasonable if also the uranyl−peroxo−carbonate complexes are considered. Interestingly, the experiments show that H_2O_2 is catalytically decomposed in the presence of uranyl−carbonate.

The experiments also show that H_2O_2 does not display any appreciable reactivity toward studtite surfaces.

Upon exposure to γ-radiation, studtite in aqueous suspension containing 10 mM HCO_3^- rapidly dissolves. The very rapid dissolution is attributed to a combination of radiolytic degradation of H_2O_2 and formation of uranyl−peroxo−carbonate complexes, keeping the concentration of free H_2O_2 at a very low level and thereby driving the dissolution process.

AUTHOR INFORMATION

Corresponding Author

*E-mail: matsj@kth.se.

ORCID

Annika C. Maier: 0000-0002-4505-0920

Mats Jonsson: 0000-0003-0663-0751

Notes

The authors declare no competing financial interest.

ACKNOWLEDGMENTS

The Swedish Nuclear Fuel and Waste Management Company (SKB) is gratefully acknowledged for financial support.

REFERENCES

(1) Kleykamp, H. The chemical state of the fission products in oxide fuels. *J. Nucl. Mater.* **1985**, *131*, 221−246.

(2) Bruno, J.; Ewing, R. C. Spent nuclear fuel. *Elements* **2006**, *2*, 343−349.

(3) Shoesmith, D. W. Fuel corrosion processes under waste disposal conditions. *J. Nucl. Mater.* **2000**, *282*, 1−31.

(4) Spinks, J. W. T.; Woods, R. J. *An Introduction to Radiation Chemistry*, 3rd ed.; John Wiley and Sons Inc.: New York, 1990.

(5) Ekeroth, E.; Roth, O.; Jonsson, M. The relative impact of radiolysis products in radiation induced oxidative dissolution of UO_2. *J. Nucl. Mater.* **2006**, *355*, 38−46.

(6) Grenthe, I.; Ferri, D.; Salvatore, F.; Riccio, G. Studies on metal carbonate equilibria. Part 10. A solubility study of the complex formation in the uranium(VI)−water−carbon dioxide (g) system at 25 °C. *J. Chem. Soc., Dalton Trans.* **1984**, 2439−2443.

(7) Gorman-Lewis, D.; Burns, P. C.; Fein, J. B. Review of uranyl mineral solubility measurements. *J. Chem. Thermodyn.* **2008**, *40*, 335−352.

(8) Clarens, F.; De Pablo, J.; Díez-Pérez, I.; Casas, I.; Giménez, J.; Rovira, M. Formation of studtite during the oxidative dissolution of UO_2 by hydrogen peroxide: a SFM study. *Environ. Sci. Technol.* **2004**, *38*, 6656−6661.

(9) Sundin, S.; Dahlgren, B.; Roth, O.; Jonsson, M. H_2O_2 and radiation induced dissolution of UO_2 and SIMFUEL in HCO_3^- deficient aqueous solution. *J. Nucl. Mater.* **2013**, *443*, 291−297.

(10) Kubatko, K. A.; Helean, K. B.; Navrotsky, A.; Burns, P. C. Stability of peroxide-containing uranyl minerals. *Science* **2003**, *302*, 1191−1193.

(11) Hanson, B. D.; McNamara, B.; Buck, E. C.; Friese, J. I.; Jenson, E.; Krupka, K.; Arey, B. W. Corrosion of commercial spent nuclear fuel. 1. Formation of studtite and metastudtite. *Radiochim. Acta* **2005**, *93* (3), 159−168.

(12) Kim, J.; Kim, H. J.; Kim, W.-S.; Um, W. Dissolution of studtite $[UO_2(O_2)(H_2O)4]$ in various geochemical conditions. *J. Environ. Radioact.* **2018**, *189*, 57−66.

(13) Burns, P. C.; Kubatko, K. A.; Sigmon, G.; Fryer, B. J.; Gagnon, J. E.; Antonio, M. R.; Soderholm, L. Actinyl peroxide nanospheres. *Angew. Chem., Int. Ed.* **2005**, *44*, 2135−2139.

(14) Lobeck, H. L.; Isner, J. K.; Burns, P. C. Transformation of uranyl peroxide studtite, $[(UO_2)(O_2)(H_2O)_2]$, to soluble nanoscale cage clusters. *Inorg. Chem.* **2019**, *58*, 6781−6789.

(15) Hickam, S.; Aksenov, S. M.; Dembowski, M.; Perry, S. N.; Traustason, H.; Russell, M.; Burns, P. C. Complexity of uranyl peroxide cluster speciation from alkali-directed oxidative dissolution of uranium dioxide. *Inorg. Chem.* **2018**, *57*, 9296−9305.

(16) Zanonato, P. L.; Di Bernardo, P.; Szabó, Z.; Grenthe, I. Chemical equilibria in the uranyl(VI)-peroxide-carbonate system; identification of precursors for the formation of poly-peroxometallates. *Dalton Trans.* **2012**, *41*, 11635−11641.

(17) Ghormley, J. A.; Stewart, A. C. Effects of γ-radiation on ice. *J. Am. Chem. Soc.* **1956**, *78* (13), 2934−2939.

(18) Hochanadel, C. J. Effects of cobalt γ-radiation on water and aqueous solutions. *J. Phys. Chem.* **1952**, *56*, 587−594.

(19) Savvin, S. Analytical use of arsenazo III Determination of thorium, zirconium, uranium and rare earth elements. *Talanta* **1961**, *8*, 673−685.

(20) Sato, T. Preparation of uranium peroxide hydrates. *J. Biochem. Toxicol.* **1963**, *13*, 361−365.

(21) Rey, A.; Casas, I.; Giménez, J.; Quiñones, J.; De Pablo, J. Effect of temperature on studtite stability: Thermogravimetry and differential scanning calorimetry investigations. *J. Nucl. Mater.* **2009**, *385*, 467−473.

(22) Burns, P. C.; Hughes, K.-A. Studtite, $[(UO_2)(O_2)(H_2O)_2]$-$(H2O)_2$: The first structure of a peroxide mineral. *Am. Mineral.* **2003**, *88*, 1165−1168.

(23) Weck, P. F.; Kim, E.; Jové-Colón, C. F.; Sassani, D. C. Structures of uranyl peroxide hydrates: a first-principles study of studtite and metastudtite. *Dalton Trans.* **2012**, *41*, 9748−9752.

(24) Guillaumont, R.; Fanghanel, T.; Fuger, J.; Grenthe, I.; Neck, V.; Palmer, D.; Rand, M. *Update on the Chemical Thermodynamics of Uranium, Neptunium, and Plutonium*, 2nd ed.; Elsevier: Amsterdam, 2003.

(25) Lobeck, H. L.; Isner, J. K.; Burns, P. C. Transformation of uranyl peroxide studtite, $[(UO_2)(O_2)(H_2O)_2](H_2O)_2$, to soluble nanoscale cage clusters. *Inorg. Chem.* **2019**, *58*, 6781−6789.

(26) Burns, P. C.; Nyman, M. Captivationwithencapsulation: a dozenyearsofexploringuranylperoxidecapsules. *Dalton Trans.* **2018**, *47*, 5916−5927.

(27) Kubatko, K. A.; Burns, P. C. Expanding the crystal chemistry of actinyl peroxides: open sheets of uranyl polyhedral in $Na_5[(UO_2)_3(O_2)_4(OH)_3](H_2O)_{13}$. *Inorg. Chem.* **2006**, *45*, 6096−6098.

(28) Lousada, C. M.; Jonsson, M. Kinetics, Mechanism, and Activation Energy of H_2O_2 Decomposition on the Surface of ZrO_2. *J. Phys. Chem. C* **2010**, *114*, 11202−11208.

(29) Lousada, C. M.; Trummer, M.; Jonsson, M. Reactivity of H_2O_2 towards different UO_2-based materials: The relative impact of radiolysis products revisited. *J. Nucl. Mater.* **2013**, *434*, 434−439.

(30) Lousada, C. M.; Yang, M.; Nilsson, K.; Jonsson, M. Catalytic decomposition of hydrogen peroxide on transition metal and lanthanide oxides. *J. Mol. Catal. A: Chem.* **2013**, *379*, 178−184.

(31) Hickam, S.; Breier, J.; Cripe, Y.; Cole, E.; Burns, P. C. Effects of H_2O_2 concentration on formation of uranyl peroxide species probed by dissolution of uranium nitride and uranium dioxide. *Inorg. Chem.* **2019**, *58*, 5858−5864.

(32) Gordon, S.; Hart, E. J.; Matheson, M. S.; Rabani, J.; Thomas, J. K. Reactionsof the hydratedelectron. *Discuss. Faraday Soc.* **1963**, *36*, 193−205.

DOI: 10.1021/acsaem.9b01611
ACS Appl. Energy Mater. 2020, 3, 352−357